Cloning and Characterization of a New Purine Biosynthetic Enzyme: A Non-Folate Glycinamide Ribonucleotide Transformylase from *E. coli*†

Ariane Marolewski, John M. Smith,‡,§ and Stephen J. Benkovic*

Department of Chemistry, The Pennsylvania State University, 152 Davey Laboratory, University Park, Pennsylvania 16802, and Seattle Biomedical Research Institute, 4 Nickerson Street, Seattle, Washington 98109

Received July 19, 1993; Revised Manuscript Received December 2, 1993®

ABSTRACT: A novel GAR transformylase has been isolated and characterized from *E. coli*. The protein, a product of the *pur*T gene, is a monomer of molecular weight 42 kDa and catalyzes the production of β-formyl GAR from formate, ATP, and β-GAR. As such it is an alternative to the formyl-folate utilizing *pur*N GAR transformylase. No significant homology exists between the two transformylases. However, the *pur*T protein shows significant homology to the *pur*K protein, also involved in purine biosynthesis. Two different *pur*T reactions have been characterized: one producing fGAR from ATP, β-GAR, and formate and the other producing acetyl phosphate and ADP from acetate and ATP. The *pur*T GAR transformylase is the first unknown *de novo* purine biosynthetic enzyme to be discovered in the last 30 years and represents another step forward in understanding cellular control of purine levels.

The broad outlines of *de novo* purine biosynthesis have been known since the late 1950s when Buchanan and co-workers (1959) outlined the 10 reactions necessary to convert phosphoribosyl pyrophosphate to inosine monophosphate. Since then research has been focused on each individual enzyme and their relationships to each other (Meyer et al., 1992; Inglese et al., 1990; Baggott et al., 1986). The first of two transformylases in this pathway act on the substrate β-GAR following the reaction shown in Scheme 1A.

Interest in *de novo* purine synthesis has been recently renewed with a view toward a deeper understanding and development of more efficacious chemotherapeutic agents (Baldwin et al., 1991; Inglese et al., 1989; Moore et al., 1990). Several anomalous results, however, suggest that *de novo* purine biosynthesis is more complicated than previously thought. An early study (Cheeseman & Crosbie, 1966; Crosbie, 1975) found that two separate *Escherichia coli* strains, one wild-type and one serine/glycine auxotroph, incorporated labeled formate at the C8 purine position. This incorporation occurred primarily under anaerobic conditions in serine-supplemented minimal media. A second later study (Dev & Harvey, 1982) using different wild-type and serine/glycine auxotrophs confirmed that formate was incorporated into the C8 position in amounts ranging from 14 to 50%. These results require an alternative GAR transformylase to be present since *E. coli* lacks a N-10 formyl folate synthase to convert formate to formyl folate for use in purine synthesis. Nygaard and Smith describe the isolation and cloning of an *E. coli* gene capable of complementing an auxotroph blocked at the GAR transformylase position (1993). This paper describes the purification and characterization of a novel GAR transformylase *E. coli* gene product which uses formate and ATP rather than formyl folate. The relevant reaction is shown in Scheme 1B.

EXPERIMENTAL PROCEDURES

Materials. The β-GAR used in the kinetic assays was synthesized according to the method of Shen (1990). ^{13}C- and ^{18}O-labeled formate, containing less than 5% ^{16}O, was obtained through the generosity of Lawrence Slieker; AIR was the generous gift of the Stubbe lab. PEI cellulose TLC plates were purchased from EM Science. Radiolabeled substrates [^{14}C]formate (specific activity 55 mCi/mmol) and [α-^{32}P]ATP (specific activity 3000 Ci/mmol) were obtained from NEN, DuPont. QAE A-25 Sephadex, DEAE Sephadex, HEPES, KCl, PMSF, $MgCl_2$, sodium formate, NADH, ATP, pyruvate kinase/lactate dehydrogenase (700 units/mL), BSA, Dalton VII molecular weight standards, and lysozyme were purchased from Sigma Chemical Co. BioGel P60 resin was obtained from Bio-Rad Laboratories. Dithiothreitol was obtained from Boehringer Mannheim and Micro-Con 30 units from Amicon. All reagents used were of the highest grade possible and were used as obtained. Kinetic measurements were made on a CARY 219 spectrophotometer. Radioactive assays were analyzed by scintillation counting using a Beckman LS8100 counter in Ecoscint fluid or quantitation on a Molecular Dynamics Phosphorimager. Nuclear magnetic resonance spectra were obtained on a Bruker WM-360.

Methods

Protein Determination. Concentrations of protein solutions were determined via Bradford protein assay. An extinction coefficient of 26.4 mM^{-1} cm^{-1} at 280 nm was calculated using BSA as a standard.

Protein Electrophoresis. SDS–polyacrylamide gel electrophoresis was performed according to the method of Laemmli (1970) on slabs of 12% polyacrylamide. The standards for molecular weight calibration were BSA, egg albumin, glyceraldehyde-3-phosphate dehydrogenase, carbonic anhydrase,

† Supported by a NSF graduate student award (A.M.), NIH Grant AI20068 (J.M.S.), and PHS Grant GM24129 (S.J.B.).

* Author to whom correspondence should be addressed.

‡ Seattle Biomedical Research Institute.

§ Present address: R&D Systems, 614 McKinley Place, N.E., Minneapolis, MN 55413.

® Abstract published in *Advance ACS Abstracts,* February 1, 1994.

[1] Abbreviations: GAR, glycinamide ribonucleotide; fGAR, β-formyl-GAR; AIR, aminoimidazole ribonucleotide; BSA, bovine serum albumin; BME, β-mercaptoethanol; PEP, phosphoenol pyruvate; NADH, nicotinamide adenine dinucleotide; DTT, dithiothreitol; PMSF, phenylmethanesulfonyl fluoride; PRA, phoshoribosylamine; fAICAR, formylaminoimidazolecarboxamide ribonucleotide; DDF, 5,8-dideazatetrahydrofolate; THF, tetrahydrofolate; PRPP, phosphoribosyl pyrophosphate; fGAM, formylglycinamidine ribonucleotide; CAIR, carboxyaminoimidazole ribonucleotide; SAICAR, succinoaminoimidazolecarboxamide ribonucleotide; AICAR, aminoimidazolecarboxamide ribonucleotide; IMP, inosine monophosphate; ZTP, AICAR triphosphate.

0006-2960/94/0433-2531$04.50/0

Scheme 1: Glycinamide Ribonucleotide Transformylase Reactions

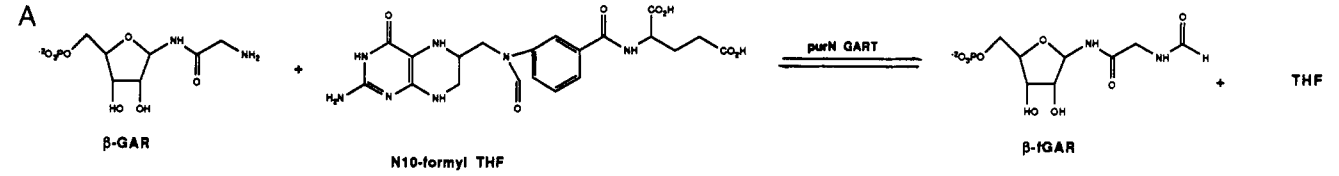

Scheme 2: Construction of pJS455

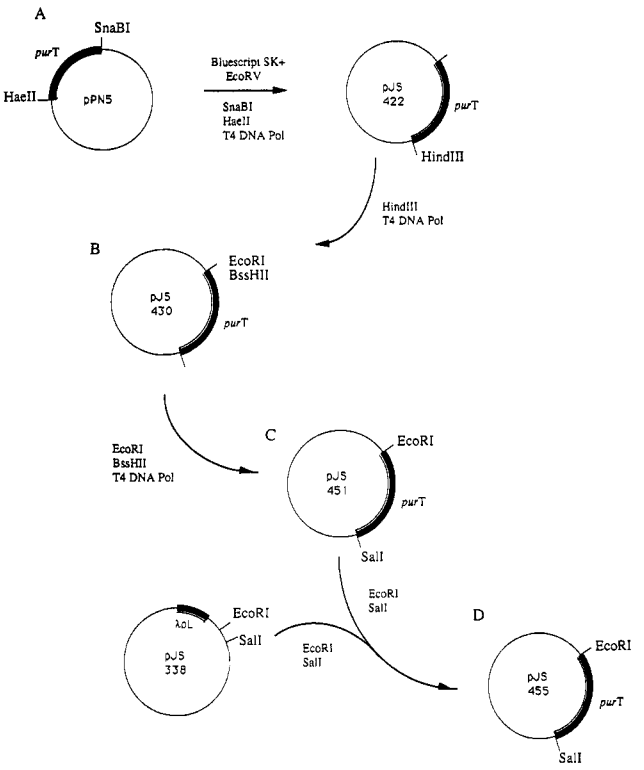

trypsinogen, trypsin inhibitor, and α-lactalbumin. Samples were denatured by boiling for 5 min in a solution of 1% SDS, 1% BME, 50 mM Tris pH 8.8, and 5% glycerol. Gels were stained for 15 min by immersion in a 1.2% Brilliant Coomassie Blue solution. Nondenaturing gels were run according to the method of Hames and Rickwood (1981) using the discontinuous high pH system buffer.

N-Terminal Sequence Analysis. Automated Edman degradation was performed on an Applied Biosystems 477A pulsed liquid sequenator. The resulting PTH derivatives were analyzed with an on-line Applied Biosystems Model 120A microbore HPLC.

Cell Strains and Construction of the PurT Expression Vector. Strain TX635 [F′ lacZ$^+$ cI857 (Mieschendahl & Muller-Hill, 1985)] contains a temperature-sensitive λ repressor and was used as a host for the λ pL plasmids. The recombinant DNA techniques employed to create this strain have been described previously (Tiedeman et al., 1985).

The *pur*T expression vector, pJS455, was created in four steps as shown in Scheme 2. (A) Plasmid vector pPN5 (Smith & Nygaard, 1993) containing a *pur*T region subclone was digested with *Sna*BI and *Hae*II and treated with T4 DNA polymerase to convert overhangs to blunt ends. This fragment was then ligated into the *Eco*RV site of Bluescript SK$^+$ (Stratagene, Inc.) and transformed into the strain XL-1 Blue on Xgal+ampicillin-selective plates. Colonies were screened by PCR to verify insert and orientation. A representative clone was selected and designated pJS422. (B) The unique *Hind*III restriction site in the Bluescript polylinker at the 3′-end of the *pur*T gene of plasmid pJS422 was eliminated by digestion with *Hind*III followed by creation of blunt ends and religation. After transformation into XL-1 Blue with selection for ampicillin resistance and verification of removal of the site, a representative plasmid was designated pJS430. (C) The wild-type *pur*T promoter and *pur*R regulatory protein binding site were removed by digestion with *Eco*RI and *Bss*HII, and religated. Plasmids containing the recreated *Eco*RI site, after ligation, were sequenced to verify *Bss*HII site removal and designated pJS451. (D) This plasmid was digested with *Eco*RI and *Sal*I enzymes and ligated into the respective sites of the λ pL expression plasmid pJS338. Following transformation into strain TX635, a representative plasmid was chosen and designated pJS455. The predicted amino acid sequence for the *pur*T protein is shown in Figure 1.

Enzyme Purification. E. coli strain TX635 containing plasmid pJS455 was grown in a rich media with ampicillin selection at 35 °C. Satisfactory levels of protein expression were achieved without formal induction, and cells were grown at 35 °C for 12 h. Cells were harvested by centrifugation, and all purification steps were carried out at 4 °C. The cells (20 g) were resuspended in 60 mL of buffer A (50 mM HEPES, 5 mM DTT pH 8.0) with 5 mg of PMSF added. Cells were lysed by addition of egg white lysozyme to 5 mg/mL and incubated on ice for 40 min. The lysate was cleared by centrifugation (12 000 rpm) for 30 min and the supernatant recovered. Streptomycin sulfate (325 mg in 10 mL of buffer A) was added to the supernatant over a period of 3 h. The suspension was then centrifuged to remove the precipitate and the supernatant (75 mL) dialyzed overnight against 2 L of buffer A.

The dialyzed supernatant was diluted 2-fold with buffer A and loaded at 2 mL/min onto a QAE A-25 Sephadex column equilibrated in the same buffer. The column was washed with approximately 200 mL of buffer until the absorbance at 280 nm was less than 0.15. A 0–0.5 M KCl gradient in 3 L of buffer A was then applied over 24 h. The GAR transformylase fractions, eluting at 0.3 M KCl, were pooled (500 mL) and concentrated to 10 mL using an Amicon ultrafiltration device. The solution was applied to a 2.5- × 54-cm BioGel P60 sizing column run at 0.08 mL/min with fractions of 2 mL collected. Active fractions were collected from the column from 80–110 mL of eluent.

```
ATG ACG TTA TTA GGC ACT GCG CTG CGT CCG GCA GCA ACT CGC GTG ATG TTA TTA
MET Thr Leu Leu Gly Thr Ala Leu Arg Pro Ala Ala Thr Arg Val MET Leu Leu

GGC TCC GGT GAA CTG GGT AAA GAA GTG GCA ATC GAG TGT CAG CGT CTC GGC GTA
Gly Ser Gly Glu Leu Gly Lys Glu Val Ala Ile Glu Cys Gln Arg Leu Gly Val

GAG GTG ATT GCC GTC GAT CGC TAT GCC GAC GCA CCA GCC ATG CAT GTC GCG CAT
Glu Val Ile Ala Val Asp Arg Tyr Ala Asp Ala Pro Ala MET His Val Ala His

CGC TCC CAT GTC ATT AAT ATG CTT GAT GGT GAT GCA TTA CGC CGT GTG GTT GAA
Arg Ser His Val Ile Asn MET Leu Asp Gly Asp Ala Leu Arg Arg Val Val Glu

CTG GAA AAA CCA CAT TAT ATC GTG CCG GAG ATC GAA GCT ATT GCC ACC GAT ATG
Leu Glu Lys Pro His Tyr Ile Val Pro Glu Ile Glu Ala Ile Ala Thr Asp MET

CTG ATC CAA CTT GAA GAG GAA GGA CTG AAT GTT GTC CCC TGC GCT CGC GCA ACG
Leu Ile Gln Leu Glu Glu Glu Gly Leu Asn Val Val Pro Cys Ala Arg Ala Thr

AAA TTA ACG ATG AAT CGC GAG GGT ATC CGT CGC CTG GCG GCA GAA GAG CTG CAG
Lys Leu Thr MET Asn Arg Glu Gly Ile Arg Arg Leu Ala Ala Glu Glu Leu Gln

CTG CCC ACT TCC ACT TAT CGT TTT GCC GAT AGC GAA AGC CTT TTC CGC GAG GCG
Leu Pro Thr Ser Thr Tyr Arg Phe Ala Asp Ser Glu Ser Leu Phe Arg Glu Ala

GTT GCT GAC ATT GGC TAT CCC TGC ATT GTA AAA CCG GTG ATG AGC TCT TCC GGC
Val Ala Asp Ile Gly Tyr Pro Cys Ile Val Lys Pro Val MET Ser Ser Ser Gly

AAG GGG CAG ACG TTT ATT CGT TCT GCA GAG CAA CTT GCT CAG GCA TGG AAG TAC
Lys Gly Gln Thr Phe Ile Arg Ser Ala Glu Gln Leu Ala Gln Ala Trp Lys Tyr

GCT CAG CAA GGC GGT CGC GCC GGA GCG GGC CGC GTA ATT GTT GAA GGC GTC GTT
Ala Gln Gln Gly Gly Arg Ala Gly Ala Gly Arg Val Ile Val Glu Gly Val Val

AAG TTT GAC TTC GAA ATT ACC CTG CTA ACC GTC AGC GCG GTG GAT GGC GTC CAT
Lys Phe Asp Phe Glu Ile Thr Leu Leu Thr Val Ser Ala Val Asp Gly Val His

TTC TGT GCA CCA GTA GGT CAT CGC CAG GAA GAT GGC GAC TAC CGT GAA TCC TGG
Phe Cys Ala Pro Val Gly His Arg Gln Glu Asp Gly Asp Tyr Arg Glu Ser Trp

CAA CCA CAG CAA ATG AGC CCG CTT GCC CTT GAA CGT GCG CAG GAG ATT GCC CGT
Gln Pro Gln Gln MET Ser Pro Leu Ala Leu Glu Arg Ala Gln Glu Ile Ala Arg

AAA GTG GTG CTG GCA CTG GGC GGT TAT GGG TTG TTT GGT GTC GAG CTA TTT GTC
Lys Val Val Leu Ala Leu Gly Gly Tyr Gly Leu Phe Gly Val Glu Leu Phe Val

TGT GGT GAT GAG GTG ATT TTC AGT GAG GTC TCC CCT CGT CCA CAT GAT ACC GGG
Cys Gly Asp Glu Val Ile Phe Ser Glu Val Ser Pro Arg Pro His Asp Thr Gly

ATG GTG ACG TTA ATT TCT CAA GAT CTC TCA GAG TTT GCC CTG CAT GTA CGT GCC
MET Val Thr Leu Ile Ser Gln Asp Leu Ser Glu Phe Ala Leu His Val Arg Ala

TTC CTC GGA CTT CCG GTT GGC GGG ATC CGT CAG TAT GGT CCT GCA GCT TCT GCC
Phe Leu Gly Leu Pro Val Gly Gly Ile Arg Gln Tyr Gly Pro Ala Ala Ser Ala

GTT ATT CTG CCA CAA CTG ACC AGT CAG AAT GTC ACG TTT GAT AAT GTG CAG AAT
Val Ile Leu Pro Gln Leu Thr Ser Gln Asn Val Thr Phe Asp Asn Val Gln Asn

GCC GTA GGC GCA GAT TTG CAG ATT CGT TTA TTT GGT AAG CCG GAA ATT GAT GGC
Ala Val Gly Ala Asp Leu Gln Ile Arg Leu Phe Gly Lys Pro Glu Ile Asp Gly

AGC CGT CGT CTG GGG GTG GCA CTG GCT ACT GCA GAG AGT GTT GTT GAC GCC ATT
Ser Arg Arg Leu Gly Val Ala Leu Ala Thr Ala Glu Ser Val Val Asp Ala Ile

GAA CGC GCG AAG CAC GCC GCC GGA CAG GTA AAA GTA CAG GGT TAA
Glu Arg Ala Lys His Ala Ala Gly Gln Val Lys Val Gln Gly *
```

FIGURE 1: Sequence of purT GAR transformylase.

Table 1: Purification of *pur*T GAR Transformylase

step	volume (mL)	protein (mg)	specific activity[a]	% yield
cell-free extract	65	280	0.10	100
strep sulfate	75	200	0.157	71
QAE A-25 Sephadex	10	100	10.6	36
P60	30	50	21	17.8
FPLC (MonoQ)	5	22	52	7.8

[a] Units/mg·mL, measured by coupled assay.

The purification of the *pur*T GAR transformylase was completed on a MonoQ HR 5/5 column (Pharmacia, FPLC). A linear gradient of 0–0.5 M KCl and 1 mM MgATP in buffer A was applied at a rate of 1%/min. The eluent was monitored at 280 nm and a central cut of the desired peak collected (at 18% gradient). Active fractions were pooled, dialyzed overnight against 50 mM HEPES with 10% glycerol, and concentrated to 9 mg/mL. Aliquots of GAR transformylase were frozen in liquid nitrogen and stored at −80 °C. The purification is outlined in Table 1.

Enzyme Assay. The *pur*T enzyme was assayed directly with radioactive substrates or indirectly via coupled assay. The direct assay monitored the conversion of [^{14}C]formate to fGAR or [α-^{32}P]ATP to ADP. A typical assay was performed in 100 mM HEPES pH 8.0, 8 mM $MgCl_2$, 1 mM ATP, 10 mM formate, 50 μM β-GAR at 25 °C. Aliquots were spotted on PEI cellulose TLC plates and run in 50 or 300 mM phosphate, pH 7.0. Radioactive compounds were visualized and quantitated via a Molecular Dynamics Phosphorimager.

The coupled assay utilizes the pyruvate kinase/lactate dehydrogenase enzyme system to monitor the production of ADP. The coupled assays were measured in 100 mM HEPES pH 8.0, 20 mM KCl, 8 mM $MgCl_2$, 1 mM ATP, 10 mM formate, 50 μM β-GAR, 2 mM PEP, 0.2 mM NADH, 80 units of pyruvate kinase/lactate dehydrogenase at 25 °C. The reaction progress was followed at 340 nm, ϵ = 6.22 mM^{-1} cm^{-1}.

Kinetics Studies: *Full Reaction.* Initial velocity studies to measure the biologically relevant reaction producing β-fGAR were performed under the constant ratio conditions of Rudolph and Fromm (1979). Rates were measured in 100 mM HEPES, 20 mM KCl pH 8.0 at 25 °C. Enzyme concentrations varied between 1 and 2 nM (stock concentration of 0.2 μM in 1% BSA). The pyruvate kinase/lactate dehydrogenase coupled assay was used and the reaction measured via NADH absorbance decrease at 340 nm. Three separate experiments were performed in which one of the three substrates was varied with the others held in a constant ratio; see Figure 2 for details.

Side Reaction. The initial rates of the side reaction, producing acetyl phosphate and ADP from acetate and ATP, were also measured via the coupled assay. Reactions were measured in 100 mM HEPES, 20 mM KCl, pH 8.0 at 25 °C. The concentration of enzyme used was 0.1 μM (stock concentration of 20 μM in 1% BSA), with acetate varying from 1 to 15 mM and ATP from 0.05 to 0.3 mM. β-GAR was not required for this reaction to occur nor did its presence at concentrations up to 0.34 mM have an effect on the rate. The data from both studies were plotted in double-reciprocal form and the kinetic parameters shown in Table 2 determined from the replots.

Metal Substitution. Rates of enzymic activity were obtained via radioactive assay in the presence of 8 mM concentrations of the following divalent metals: Mg, Mn, Co, Ni, Zn, and Cu. All metals were added as the chloride salts. Reaction in the absence of metal served as a control.

β-GAR Synthesis and Purification. β-GAR was synthesized according to the method of Shen (1990) in a reaction using ATP, PRA, glycine, and crude GAR synthetase. The completed reaction was diluted 10-fold into 10 mM NH_4OAc pH 3.0. This solution was then loaded onto a DEAE Sephadex column (2.5 × 20 cm) equilibrated in the same buffer at 4 °C. The flow through from this column was collected, lyophilized, and resuspended in 10 mL of 10 mM NH_4OAc pH 9.0. This sample was applied to a DEAE column equilibrated in the same buffer and eluted with a 0–1 M acetic acid gradient. Relevant fractions, eluting at a pH of 4, were quickly pooled and repeatedly lyophilized from distilled water. The β-GAR produced was quantitated using the *pur*N GAR transformylase and 10-formyl-5,8-dideazafolate ($\Delta\epsilon$ = 18.5 mM^{-1} cm^{-1} at 295 nm). This enzyme is specific for the β-anomer of GAR. Total phosphate determination (Ames & Dubin, 1960) was also performed on each sample. The amount of contaminating α-GAR was determined by subtracting β-GAR concentrations from total phosphate. All GAR used in the kinetic assays was >90% β-anomer.

Enzymatic Synthesis of fGAR. [^{14}C]fGAR was synthesized for use in measuring the equilibrium constant. The synthesis was accomplished using the *pur*T GAR transformylase and ^{14}C-labeled formate. The reaction mixture consisted of 2 mM $MgCl_2$, 1 mM formate, 1 mM ATP, 1.3 mM β-GAR, and 85 nM *pur*T GAR transformylase in 50 mM HEPES pH 8.0. [^{14}C]fGAR was purified by SAX HPLC in 50 mM formate buffer at isocratic gradient. The purified fGAR was lyophilized repeatedly from distilled water to remove formate.

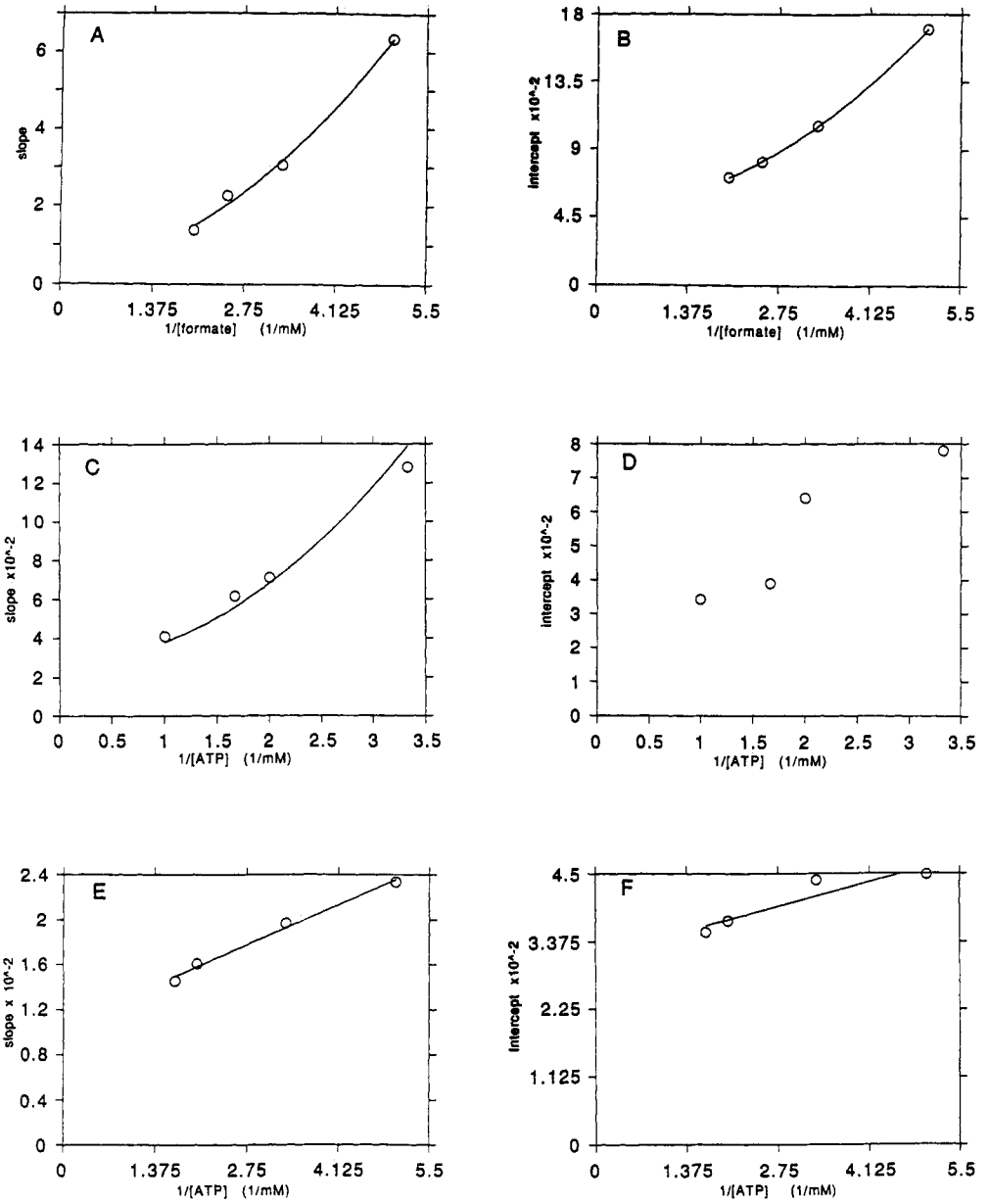

FIGURE 2: Secondary plots of slope or intercept versus reciprocal concentration of one of the varied substrates. (A and B) Replots from experiment varying ATP at a formate/GAR ratio of 20; 0.5 < [ATP] < 0.3 mM, 0.2 < [formate] < 0.5 mM, 10 < [GAR] < 25 μM. (C and D) Replots from experiment varying GAR at an ATP/formate ratio of 1.0; 5 < [GAR] < 30 μM, 0.3 < [formate] < 1.0 mM, 0.3 < [ATP] < 1.0 mM. (E and F) Replots from experiment varying formate at an ATP/GAR ratio of 20; 0.2 < [formate] < 1 mM, 10 < [GAR] < 30 μM, 0.2 < [ATP] < 0.6 mM.

Table 2: Kinetic Constants of *pur*T GAR Transformylase

substrate	pH	k_{cat} (s^{-1})	K_m (μM)
		Full Reaction	
formate	8.0	37.6 ± 0.810	319 ± 14.6[a] (252 ± 63)[b]
β-GAR	8.0		10.1 ± 0.51 (14 ± 6.3)
ATP	8.0		nondefined[a] (45 ± 12.6)
		Side Reaction	
acetate	8.0	0.309 ± 0.0358	3.68 mM ± 0.424
ATP	8.0		77.4 μM ± 24

[a] Determined graphically. [b] Determined via computer fitting.

Equilibrium Constant $[ADP][P_i][fGAR]/[ATP] \times [HCOOH][GAR]$. Reactions consisting of ADP, inorganic phosphate, [^{14}C]fGAR, and 1 nM *pur*T GAR transformylase were allowed to come to equilibrium over 3 h at 25 °C. At various intervals, aliquots were removed and analyzed on PEI cellulose plates (relative migration of formate = 0.56, fGAR = 0.37in 50 mM phosphate at pH 7.0). The equilibrium constant was calculated via the above formula after determining the amount of formate and fGAR present and assuming a 1:1 stoichiometry of formate and ATP. Reactions were performed with 10 and 5 mM added ADP and inorganic phosphate. These concentrations were chosen to force the final ratio of fGAR to formate to be approximately 5, allowing for more accurate quantitation. Measurement of the equilibrium constant from the forward direction was not possible due to sensitivity problems.

Stoichiometry of the purT Reactions. The stoichiometry of the full reaction producing β-fGAR was evaluated through double label assays in which [^{14}C]formate and [α-^{32}P]ATP were incubated with unlabeled β-GAR at concentrations of ATP, formate, and β-GAR between 0.1 and 0.5 mM. The products, [^{14}C]fGAR and [α-^{32}P]ADP, were then separated by PEI cellulose TLC as described under enzyme assay and quantitated on a Molecular Dynamics Phosphorimager.

Table 3: Possible Alternative Substrates for *pur*T

formyl acceptor	formyl donor	NTP	metal	specific activity[a]
β-GAR	formate	ATP	Mg	52
α-GAR				
β-GAR	10-formyl-DDF	ATP		
	5-formyl-THF			
	fAICAR			
	formylmethionine			
	formiminoglutamate			
β-GAR		GTP		
		CTP		
		TTP		
		ITP		
		ZTP		
β-GAR	formate	ATP	Mn	2.6
			Co	17.3
			Zn	
			Cu	
			Ni	

[a] Units/mg·mL.

Scheme 3: Alternative Order of Binding for *pur*T GAR Tfase

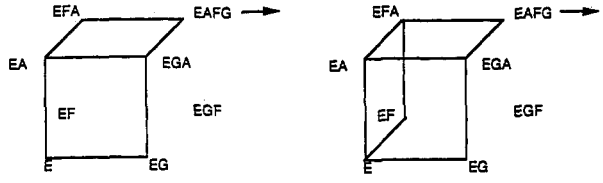

Relative migration values are as follows: formate = 0.83, fGAR = 0.79, ADP = 0.50, ATP = 0.30.

The stoichiometry of the side reaction requiring ATP and acetate was evaluated by comparing the ADP produced to the acetyl phosphate trapped. The coupled assay was used to measure ADP whereas acetyl phosphate was quantitated after trapping as a hydroxamate, as detailed under acyl phosphate detection.

Detection of Acyl Phosphates. The presence of acyl phosphates was determined by conversion to the hydroxamate according to the method of Pechere and Capony (1967). The absorbance at 490 nm was compared to a succinohydroxamate standard for calibration. Time courses of acyl phosphate production were measured for both full reaction (formate, ATP, and GAR) and side reaction (acetate and ATP).

Nuclear Magnetic Resonance Spectroscopy. ^{31}P NMR spectra were collected at 145.8 MHz on a Bruker Instruments Inc. WM-360. Reactions in 10 mM HEPES containing 2 mM MgATP, 1 mM labeled formate, 1.3 mM β-GAR, and 85 nM *pur*T GAR transformylase were incubated at room temperature for 3 h. The samples were then treated with a small amount of Chelex to remove Mg^{2+}, taken to dryness, and resuspended in 0.5 mL of D_2O. Field frequency locking to ^2H was maintained by using D_2O as a solvent. The sweep width was set at 29 411 Hz at ambient probe temperature with broad-band proton decoupling. The total number of scans was 7944 with 32K data points. The phosphate peak was identified by comparison with an internal standard.

RESULTS AND DISCUSSION

Physical Properties. *pur*T GAR transformylase is a single subunit protein of 392 amino acids with a molecular weight of 42 400 as deduced from the predicted amino acid sequence. The approximate molecular weight of 41 900 obtained by SDS-PAGE is thus in good agreement. Behavior on nondenaturing gels and sizing columns during the purification suggests that the enzyme exists as a monomer under both reducing and nonreducing conditions. The N-terminal sequence has been determined by automated Edman degradation and corresponds to the sequence predicted from the gene.

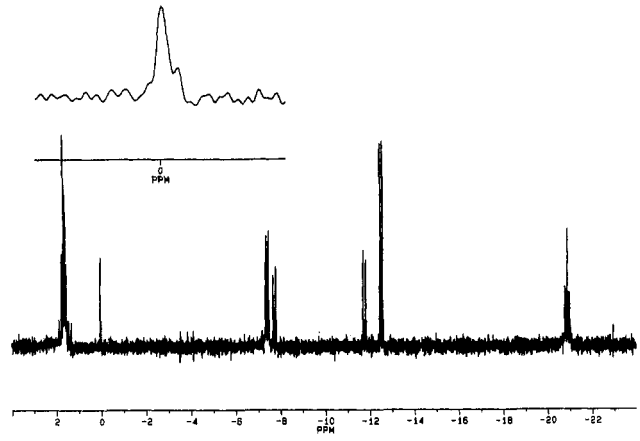

FIGURE 3: ^{31}P NMR spectrum of [$^{16}O/^{18}O$] inorganic phosphate produced by *pur*T GAR transformylase. See the Experimental Procedures for further details.

MTLLGTALRPAATRVMLLGS (gene)

TLLGTALRPAATRVMLLGS (protein)

Enzyme Specificities. The stoichiometry of the full reaction has been determined through double labeling studies to be 1:1:1. The *pur*T enzyme utilizes only the biologically relevant β-isomer of GAR in keeping with its presumed role as a viable alternative *in vivo*. This specificity extends to the other two substrates as well, with no other NTP or formyl donor tested able to substitute for ATP or formate. However, the requirement for divalent metals is less stringent since cobalt and manganese are able to substitute *in vitro* for magnesium. A gene labeled as *pur*U has recently been isolated (Nagy et al., 1993) which may hydrolyze formyl-THF to produce formate. This would provide a source of formate in aerobically grown *E. coli* and allow the *pur*T transformylase to function at a higher level. The ability of *pur*T GAR transformylase to function with a variety of metals is in accordance with results from other enzymes such as PEP carboxylase which also require magnesium (O'Leary et al., 1981). Table 3 details the various substrates tested with the enzyme. The equilibrium constant for the forward reaction was measured as $(2.0 \pm 0.35) \times 10^6$ at 25 °C, reflecting the low reversibility of reactions in which ATP is cleaved.

Steady-State Kinetics. The *pur*T GAR transformylase catalyzes two distinct reactions. The first of these, the full reaction, is the biologically relevant transformation of β-GAR into fGAR. The second, or side reaction, is the cleavage of ATP in the presence of acetate to generate acetyl phosphate and ADP.

Initial rate studies for a ter-reactant mechanism allow distinctions to be made between various sequential and Ping-Pong mechanisms (Fromm & Rudolph, 1979). Three initial rate studies were performed on the full *pur*T reaction, varying one substrate while maintaining the others in a constant ratio. The data generate three intersecting patterns when plotted in a double-reciprocal form, characteristic of a sequential mechanism. The six secondary replots, slope and intercept versus reciprocal concentration, are shown in Figure 2A–F.

The kinetic parameters were determined by extrapolation of the replot to infinite concentration and are reported in Table

Scheme 4: Transfer of Formate Oxygen to Phosphate

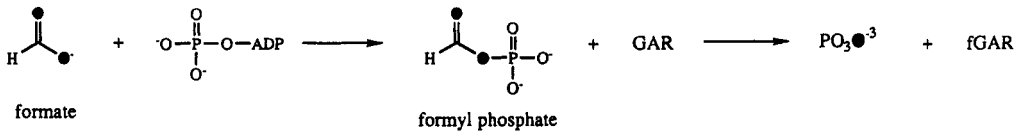

2. Extrapolations of the intercept replots (Figure 2B,D,F) provide $(V_{max})^{-1}$ values, and likewise, extrapolation of slope replots (Figure 2A,C,E) provide K_m/V_{max} for the varied substrates. These constants were verified in a separate experiment by measuring the initial rates in the presence of saturating concentrations of two of the three substrates, the third being varied. These rates were fit to Cleland's HYPERO program (and the results also shown in Table 2). The two methods generate values that are in reasonable agreement. An operational definition of the Michaelis constant for ATP (the concentration to reach half of V_{max}) is obtainable from the fitting program but not in terms of the combination of ATP with EGF since its concentration is zero (Figure 2A). The specific activity of 52 μg/min·mg·mL as well as the K_m value of 10.1 μM for β-GAR are comparable to those of the *pur*N GAR transformylase (specific activity = 14 μmol/min·mg·mL, K_m β-GAR = 12 μM at pH 7.5). This again supports the hypothesis that the *pur*T GAR transformylase is capable of substituting *in vivo* for the tetrahydrofolate requiring transformylase.

The choice of a mechanism can be limited by considering the behavior of the replots. Both the slope and intercept replot for the study varying ATP (Figure 2A,B) are parabolic with the slope replot intersecting at the origin. The replots for the study varying GAR are also parabolic but have nonzero intercepts (Figure 2C,D). The two replots from the study varying formate (Figure 2E,F) can be fit linearly and do not contribute to a choice of mechanism. The two mechanisms that display this behavior are diagrammed in Scheme 3. Both potential mechanisms contain the random sequential binding of ATP, formate, and β-GAR with the omission of one or more possible complexes.

The binding of all three substrates may be followed by the formation of a tightly bound formyl phosphate intermediate and ADP, as suggested by the NMR data and by analogy to acetyl phosphate production.

The side reaction is noteworthy in two respects. The rate of ATP cleavage in the presence of acetate is only 100-fold less than that in the full reaction, yet cleavage of ATP in the presence of formate is undetectable. The side reaction provides an analogy to the mechanism of the full reaction, supporting the idea of a tightly bound formyl phosphate intermediate in the latter. The ratio of acetyl phosphate trapped to ADP produced is 0.701 ± 0.15, demonstrating that acetate and ATP react with less than equivalent stoichiometry in the side reaction compared to formate and ATP in the full reaction. In the presence of β-GAR there is no formation of acetyl-GAR. The acetyl phosphate unaccounted for is likely hydrolyzed either at the active site or in solution before being trapped despite our efforts to maximize the latter's efficiency. The K_m for ATP in the side reaction is 65 μM, which is comparable to that for the full reaction, indicating that both processes probably occur at the same ATP binding site.

No free formyl phosphate was detected in any studies of the full reaction; however, this could be explained by tighter binding in the active site or lack of accumulation. Any formyl phosphate produced in the full reaction is turned over to fGAR, whereas acetyl phosphate undergoes no further enzymic reactions and is released into solution to become available to trap. Experiments are in progress to test for burst production of formyl phosphate in the presence of ATP and formate.

Table 4: Partial Reactions of *pur*T GAR Transformylase

formyl acceptor	formyl donor	NTP	specific activity[a]
	formate	ATP	
β-GAR		ATP	
β-GAR	formate		
	acetate[b]	ATP	0.42
β-GAR	bicarbonate[c]	ATP	
AIR	formate	ATP	
AIR	bicarbonate	ATP	

[a] Units/mg·mL. [b] At concentrations up to 10 mM. Substitutions of acetamide, trifluoroacetate, chloroacetate, carbamate, sulfamate, and propionate were inactive. [c] Concentrations up to 15 mM.

Nuclear Magnetic Resonance Spectroscopy. The substitution of ^{18}O for ^{16}O causes an upfield isotopic shift on the signal of the ^{31}P atom bound to that oxygen (Cohn & Hu, 1978). This shift is approximately 0.02 ppm for a phosphorus oxygen bond. Figure 3 shows a portion of the ^{31}P NMR spectrum obtained from a *pur*T GAR transformylase catalyzed reaction using ^{18}O-labeled formate. The two peaks corresponding to P–^{16}O and P–^{18}O are separated by 0.02 ppm and are in a 3:1 ratio, indicating that transfer of one formate oxygen into phosphate has occurred.

The NMR study demonstrates that the *pur*T GAR transformylase reaction proceeds through a transfer of atomic oxygen from formate to the γ-phosphoryl moiety of ATP. One interpretation is the intermediacy of formyl phosphate (Scheme 4) whose presence is also supported by the identification of *acetyl* phosphate as a product in the side reaction.

Homology. There is no significant homology between the two GAR transformylases, a reasonable expectation given their different formyl donors and presumably different mechanisms. The *pur*T protein does, however, display significant homology to the *pur*K gene product, a subunit of aminoimidazole ribonucleotide carboxylase (27% exact and 55% conserved). Yet the *pur*T enzyme does not use any of the *pur*K substrates either singly or in combination, as seen in Table 4. Although these two enzymes may be evolutionarily related, the active sites have become very specific; formate vs bicarbonate and GAR vs AIR. The possible evolutionary relationship between these two proteins is intriguing and should be further explored.

CONCLUSION

A novel GAR transformylase has been discovered and isolated from *E. coli*. This is the first new enzyme in *de novo* purine biosynthesis to be discovered in 30 years. Its presence in *E. coli* will allow a better understanding of the relationships between various purine biosynthetic enzymes and maintenance of fGAR levels. Preliminary results (Warren, unpublished) suggest this enzyme is present in higher organisms allowing the development of potential chemotherapeutic agents which block this activity.

ACKNOWLEDGMENT

We thank C. Falzone for his assistance with the NMR experiments and M. Warren for his critical reading of the manuscript.

REFERENCES

Ames, B. N., & Dubin, D. T. (1960) *J. Biol. Chem. 235*, 769–775.
Baggott, J. E., Vaughn, W. H., & Hudson, B. B. (1986) *Biochem. J. 236*, 193–200.
Baldwin, S. W., Tse, A., Gossett, L., Taylor, E. C., Rosowsky, A., Shih, C., & Moran, R. G. (1991) *Biochemistry 30*, 1997–2006.
Buchanan, J. M., & Hartman, S. C. (1959) *J. Biol. Chem. 234*, 1812–1816.
Cheeseman, P., & Crosbie, G. W. (1966) *Biochem. J. 99*, 24.
Cleland, W. W. (1979) *Methods Enzymol. 63*, 103–138.
Cohn, M., Hu, A. (1978) *Proc. Natl. Acad. Sci. U.S.A. 75*, 200–203.
Crosbie, G. M. (1975) *Biochem. Soc. Trans. 3*, 1255–1156.
Dev, I. K., & Harvey, R. J. (1982) *J. Biol. Chem. 257*, 1980–1986.
Hames, B. D., & Rickwood, D. (1981) in *Gel Electrophoresis of Proteins*, pp 23–40 IRL Press, Oxford.
Inglese, J., Blatchly, R. A., & Benkovic, S. J. (1989) *J. Med. Chem. 32*, 937–940.
Inglese, J., Smith, J. M., & Benkovic, S. J. (1990) *Biochemistry 29*, 6678–6687.
Laemmli, U. K. (1970) *Nature (London) 227*, 680–685.
Meyer, E., Leonard, N. J., Bhat, B., Stubbe, J., & Smith, J. M. (1992) *Biochemistry 31*, 5022–5032.
Mieschendahl, M., & Muller-Hill, B. (1985) *J. Bacteriol. 164*, 1366–1369.
Moore, E. C., Hurlbert, R. B., & Massia, S. P. (1990) *Biochem. Pharmacol. 38*, 4037–4044.
Nagy, P. L., McCorkle, G. M., & Zalkin, H., personal communication.
Nygaard, P., Smith, J. M., *J. Bacteriol.* (in press).
O'Leary, M. H., Rife, J. E., & Slater, J. D. (1981) *Biochemistry 20*, 7308–7314.
Pechere, J. F., & Capony, J. F. (1967) *Anal. Biochem. 22*, 536–553.
Rudolph, F. B., & Fromm, H. J. (1979) *Methods Enzymol. 63*, 138–159.
Shen, Y., Rudolph, J., Stern, M., Stubbe, J., Flanigan, K. A., & Smith, J. A. (1990) *Biochemistry 29*, 218–227.
Smith, J. M., & Nygaard, P. (1993) *Mol. Microbiol.* (manuscript submitted).
Tiedeman, A. A., Smith, J. M., & Zalkin, H. (1985) *J. Biol. Chem. 260*, 8676–8679.